Broad-Band Microwave Measurement of Water Using Transient Radiation

C. David Capps, R. Aaron Falk, Stuart G. Ferrier, and Tim R. Majoch, *Member, IEEE*

Abstract—**Previous workers have demonstrated the utility of optoelectronically pulsed antennas to make broad-band microwave measurements of the dielectric properties of relatively low loss materials. This work presents an extension of the analysis technique that allows measurements to be made on highly absorptive samples. Experimental results for water in the 10–70 GHz frequency range are presented, error sources analyzed, and results compared with measurements made with a different technique.**

I. Introduction

RECENTLY, it has been shown that transient radiation from optoelectronically pulsed antennas can be used to measure the complex permittivity for relatively lossless solids in the microwave frequency region [1]. In this work we will show that the technique can be extended to measure the permittivity, or equivalently, the complex refractive index of a very lossy liquid, e.g., water. The principal difference is that for low loss materials, the sample can be made thick enough that multiple reflections can be removed by time windowing. For highly absorptive media the samples must be very thin to transmit measurable energy and an alternative method used for analysis.

The paper is organized as follows. First, we briefly review the experimental apparatus for the coherent microwave transient spectroscopy technique and describe the liquid sample cell. We will then develop the theory necessary to analyze the data. Finally, results will be presented, along with an analysis of uncertainties, and compared with measurements using the method of travelling waves [2].

II. Experimental Apparatus

The experimental setup is shown in Fig. 1. The exponentially tapered transmitter and receiver antennas have been described extensively in the literature [1], [3]–[5]. Our antennas are 7.9 mm long with a horn width of 2.6 mm. A mode locked dye laser operating at approximately 600 nm generates the 2.7 ps pulses which are split to form the pump and probe pulses. The pump beam is mechanically chopped and the intensity monitored by the photoconductive response of the transmitter so that laser power fluctuations can be factored into the data processing. The optoelectronically generated microwave radiation is collimated by a 37 mm diameter fused silica hemispherical lens. An identical lens is used to focus the transmitted beam onto the receiver. Fused silica was chosen as measurement [5] showed the complex refractive index to be nearly constant over the frequency region of interest. The translation stage and the lock-in amplifiers are computer controlled so that the data collection process is fully automated. Fig. 2 shows a typical received pulse and the magnitude of its Fourier transform. For our apparatus, the useful frequency range is from approximately 10 to 70 GHz. Other workers [1] have shown larger bandwidths with this technique. However, absorption in the stripline of our antennas limited our useful bandwidth to the stated range.

In order to extract the complex index of refraction from transmission data, it is necessary to measure the transmitted field for different sample thicknesses. Calculations using published values [2] for the index of water indicated that we would obtain measureable signals only for sample thicknesses less than 1 mm. Fig. 3 shows the design of the sample cell which allowed variation of sample thickness from 0.100 to 1.0 mm. Uncertainty in sample thickness was 0.045 mm which includes both variation in window thickness and window tilt across the area covered by the microwave beam. Fused silica was used as the window material due to its relatively uniform index in the experimental frequency range.

III. Theory

Fig. 4 shows the sample and cell configuration to be analyzed. A linearly polarized electromagnetic field $E(t)$ is normally incident on the plane parallel slabs and propagates in the $+z$ direction. We will assume the materials are nonmagnetic, i.e., $\mu = 1.0$, and isotropic. The frequency dependent, complex index of refraction N is related to the complex permittivity ϵ by

$$N(\omega) = \sqrt{\epsilon(\omega)} \equiv n(\omega) + ik(\omega). \tag{1}$$

The incident frequency components ${}_{+}E_1(\omega)$ are obtained from the Fourier transform of the incident field $E(t)$

$${}_{+}E_1(\omega) = \int_{-\infty}^{\infty} E(t)\, e^{i\omega t}\, dt \tag{2}$$

Manuscript received March 6, 1991; revised September 12, 1991.

The authors are with Boeing Defense & Space Group, Aerospace & Electronics Division, P.O. Box 3999, Seattle, WA 91824.

IEEE Log Number 9104479.

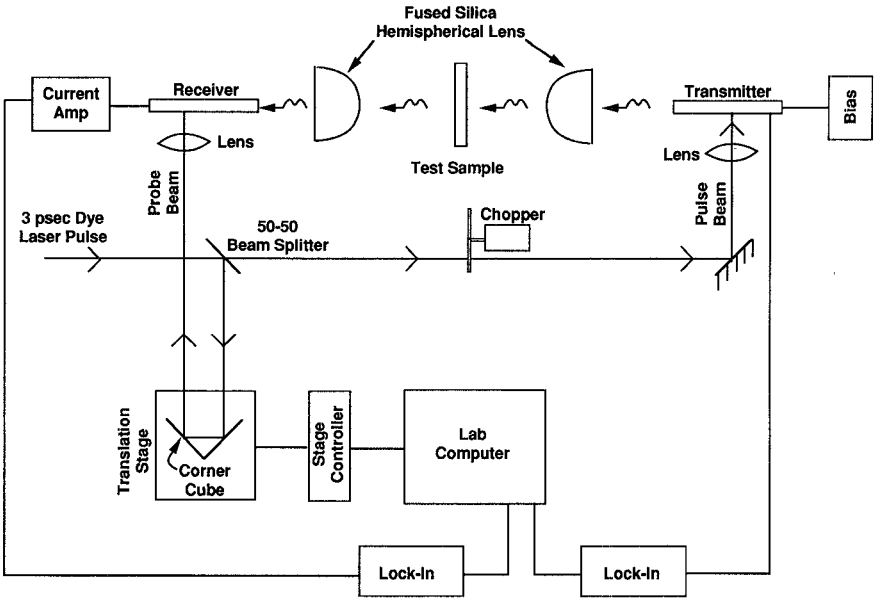

Fig. 1. Experimental setup for coherent microwave transient spectroscopy.

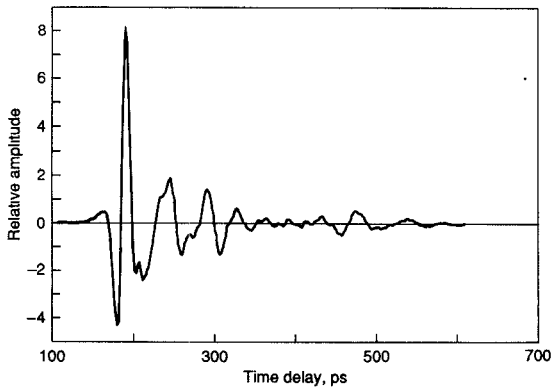

(a)

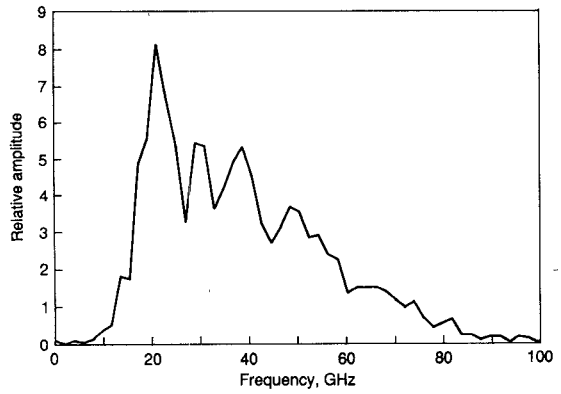

(b)

Fig. 2. (a) Time delay scan for a typical pulse. (b) Magnitude of the Fourier transform of a typical pulse.

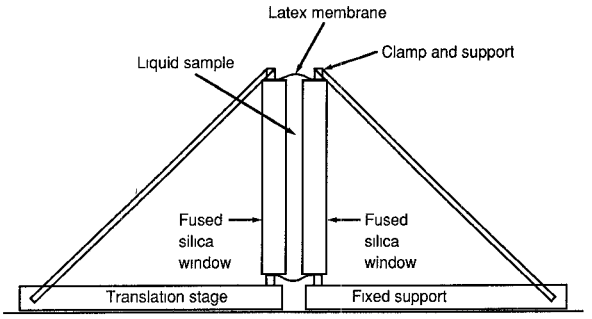

Fig. 3. Liquid sample cell.

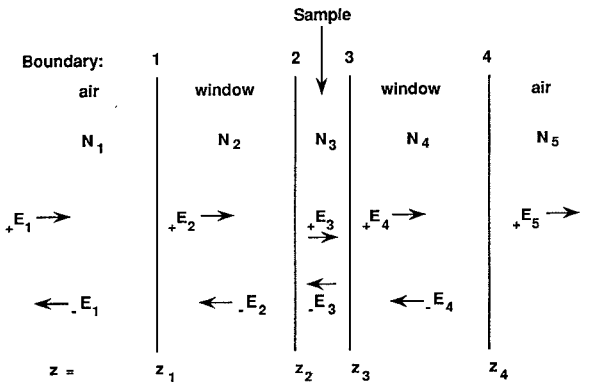

Fig. 4. Sample cell boundary and field notation.

and transmitted field components $_{+}E_5(\omega)$ are, likewise, determined from the measured received pulse $E_m(t)$

$$_{+}E_5(\omega) = \int_{-\infty}^{\infty} E_m(t)\, e^{i\omega t}\, dt. \tag{3}$$

The transmitted field components may be expressed in terms of $_{+}E_1$ and N_j by solving the set of linear equations generated by the boundary conditions (continuity of tangential electric and magnetic fields) at Boundaries 1–4. Boundary conditions at each interface can be conveniently written as a matrix equation relating the fields on the right side of the boundary to those on the left. If the "+" subscript denotes waves propagating in the positive z-direc-

tion and "−" in the negative, then the boundary conditions for the first three boundaries can be written

$$\begin{pmatrix} {}_{+}E_{I+1} \\ {}_{-}E_{I+1} \end{pmatrix} = A(I) \begin{pmatrix} {}_{+}E_{I} \\ {}_{-}E_{I} \end{pmatrix} \tag{4}$$

where

$$A(I) = \begin{pmatrix} \left(\frac{N_{I+1} + N_I}{2N_{I+1}}\right) \exp\left\{-i\frac{\omega(N_{I+1} - N_I)z_I}{c}\right\} & \left(\frac{N_{I+1} - N_I}{2N_{I+1}}\right) \exp\left\{-i\frac{\omega(N_{I+1} + N_I)z_I}{c}\right\} \\ \left(\frac{N_{I+1} - N_I}{2N_{I+1}}\right) \exp\left\{i\frac{\omega(N_{I+1} + N_I)z_I}{c}\right\} & \left(\frac{N_{I+1} + N_I}{2N_{I+1}}\right) \exp\left\{i\frac{\omega(N_{I+1} - N_I)z_I}{c}\right\} \end{pmatrix}. \tag{5}$$

The final boundary equations have a slightly different form as there is not a negative propagating field to the right of this boundary. The matrix equation for this interface is thus

$$\begin{pmatrix} {}_{+}E_{5} \\ {}_{+}E_{5} \end{pmatrix} = B \begin{pmatrix} {}_{+}E_{4} \\ {}_{-}E_{4} \end{pmatrix} \tag{6}$$

where

$$B = \begin{pmatrix} \exp\left\{-i\frac{\omega(N_5 - N_4)z_4}{c}\right\} & \exp\left\{-i\frac{\omega(N_5 + N_4)z_4}{c}\right\} \\ \left(\frac{N_4}{N_5}\right) \exp\left\{-i\frac{\omega(N_5 - N_4)z_4}{c}\right\} & -\left(\frac{N_4}{N_5}\right) \exp\left\{-i\frac{\omega(N_5 + N_4)z_4}{c}\right\} \end{pmatrix}. \tag{7}$$

The matrix C given by

$$C = B \cdot A(3) \cdot A(2) \cdot A(1) \tag{8}$$

relates the transmitted field to the fields to the left of the cell. Denoting the elements of C by c_{ij} and solving yields

$${}_{+}E_5 = {}_{+}E_1 \frac{c_{22}c_{11} - c_{12}c_{21}}{c_{22} - c_{12}}. \tag{9}$$

If the first interface is taken as the coordinate origin, i.e., $z_1 = 0$, the window thickness as d, and the thickness of the jth sample as h_j, then

$$\begin{aligned} z_2 &= d \\ z_3 &= d + h_j \\ z_4 &= 2d + h_j \end{aligned} \tag{10}$$

and (9) becomes an explicit function of the sample thickness. If the incident pulse form is constant, then the incident field can be eliminated from (9) by measuring the transmitted field for two different thicknesses and dividing:

$$\frac{{}_{+}E_5(h_2)}{{}_{+}E_5(h_1)} = \frac{[c_{22}(h_1) - c_{12}(h_1)]\,[c_{22}(h_2)c_{11}(h_2) - c_{12}(h_2)c_{21}(h_2)]}{[c_{22}(h_2) - c_{12}(h_2)]\,[c_{22}(h_1)c_{11}(h_1) - c_{12}(h_1)c_{21}(h_1)]}. \tag{11}$$

Attempts at analytic inversion of (11) to obtain the complex refractive index of the sample in terms of the other parameters have not been successful. The left side of (11) is a complex number, i.e., two real numbers, obtained from the experimental measurements of two different sample thicknesses. The right hand side is a function of two unknowns, the real and imaginary parts of the complex index of the sample material. Thus, (11) may be thought of as two equations in two unknowns. If an additional sample is measured and the field component divided by one of the previously determined components, then two more equations in the same unknowns are created. Obviously, this procedure can be extended to create a system of $2N$ equations in two unknowns. Such an overdetermined system can be solved numerically in a least squares sense. We, therefore, measure the transmitted field for M different sample thicknesses and minimize the sum of squares

$$S = \sum_{J=2}^{M} \left| \frac{{}_{+}E_5(h_j)}{{}_{+}E_5(h_1)} - \frac{[c_{22}(h_1) - c_{12}(h_1)]\,[c_{22}(h_j)c_{11}(h_j) - c_{12}(h_j)c_{21}(h_j)]}{[c_{22}(h_j) - c_{12}(h_j)]\,[c_{22}(h_1)c_{11}(h_1) - c_{12}(h_1)c_{21}(h_1)]} \right|^2 \tag{12}$$

with respect to N_3 to determine the complex refractive index of the sample.

IV. Results and Discussion

The complex refractive index for the window material, N_2 and N_4, appears in (5) and (7). Thus, before proceeding with the measurement on water we determined the refractive index of the fused silica windows, both as a check on the apparatus and to use in the analysis of the water data. Three 1.0 cm thick optical quality, fused silica windows were obtained from one supplier. Samples of different thickness were obtained by stacking one, two or three plates in a clamping fixture. The plate flatness and the wavelength of the highest frequency considered, 70 GHz, yield the result that the gap between slabs is less than $\lambda/100$, suppressing interface reflections. This suppression is supported by examination of the data where pulses

reflected from the external surfaces are clearly visable but nothing exceeding the noise level is visible at positions expected for pulses reflected by internal interfaces.

Two time delay scans for each of three sample thicknesses, 1.0, 2.0, 3.0 cm, were taken. Each of the 2^3 combinations was analyzed using (12) modified for the air-sample-air case to obtain n and k. The means and the standard deviations of these values estimate the real and imaginary parts of the refractive index and the uncertainties due to random noise in the apparatus. Contribution of the thickness uncertainty, 0.025 mm per slab (added in quadrature for stacked samples), to the index uncertainty was determined by Monte Carlo analysis. Normally distributed, zero mean errors drawn from distributions with the standard deviations for each sample thickness were added to the nominal thickness and the analysis repeated. No significant increase in the standard deviation of n and k was observed, indicating noise dominated the thickness uncertainty effects. Plotting n and k versus frequency showed a periodic oscillation superimposed on approximately linear trends. The period of this oscillation corresponds closely to the time it takes a signal to travel from the point on the receiver antenna stripline, where the probe pulse strikes, to the end of the stripline and back to the probe point. We, thus, attribute this periodic oscillation to signal contamination resulting from reflections off the back of the antenna. The standard deviations were increased by adding a frequency independent term in quadrature to the previously determined uncertainties to account for this systematic error effect. The magnitude of the term was determined by requiring that the chi-square per degree of freedom for a linear fit be equal to 1.0. Averaged over the frequency region, the ratio of the uncertainties due to the random errors and to the reflection effect is 0.35. Figs. 5 and 6 show n and k, respectively, with one standard deviation error bars.

Also shown in Figs. 5 and 6 are the plus and minus one standard deviation lines from the fused silica measurements of Pastol *et al.* [5]. Values shown were calculated from the plotted data in their Fig. 5 using linear interpolation between data points. While the statistical agreement is good, the systematic increase in the absorption coefficient around 20 GHz is absent in our results. Pastol *et al.*, attribute this absorption increase to the residual water content of the sample. Thus, the difference may be explained by the differing water content of samples obtained from different sources.

A smoothed index for the window material was obtained by separately fitting the real and imaginary parts of the index with straight lines. The results are shown in Figs. 7 and 8 along with the 68% confidence intervals for the fit. In the error analysis for the water measurements these confidence limits will be used as the one standard deviation errors for the window index.

Distilled water was placed in the sample cell and two time delay scans were made for each of the nominal thicknesses 0.3 through 1.0 mm in 0.1 mm increments. A random sample of 15 of the 2^8 possible data combinations

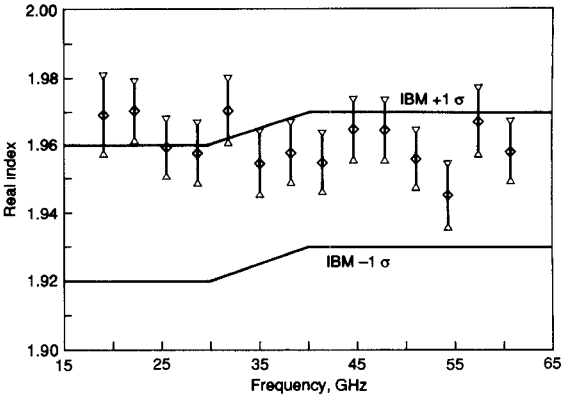

Fig. 5. Real part of complex refractive index for fused silica.

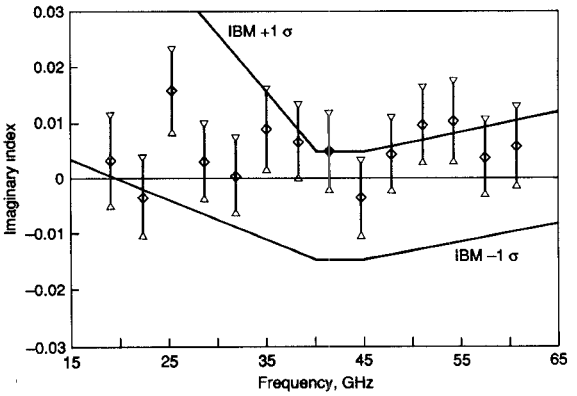

Fig. 6. Imaginary part of complex refractive index for fused silica.

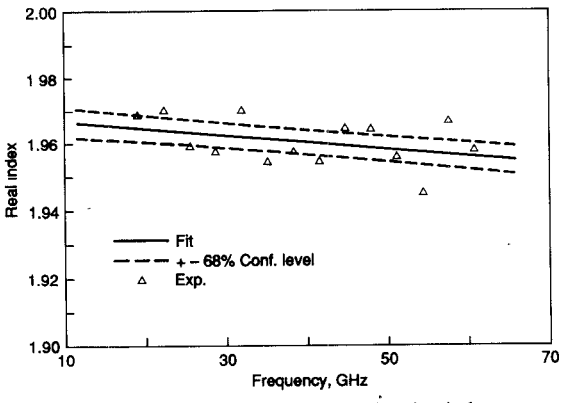

Fig. 7. Linear fit to real part of refractive index.

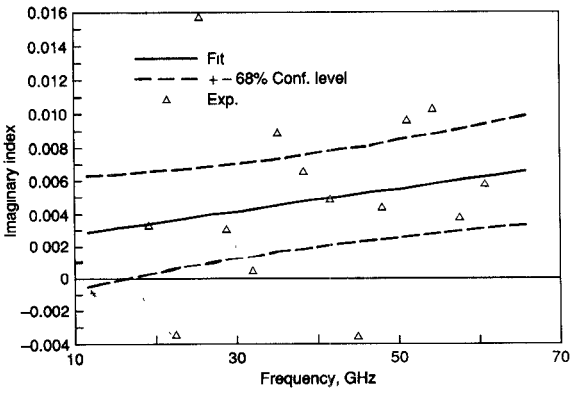

Fig. 8. Linear fit to imaginary part of refractive index.

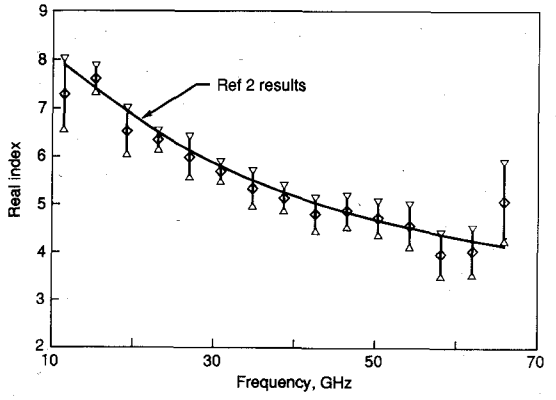

Fig. 9. Real part of complex refractive index for water.

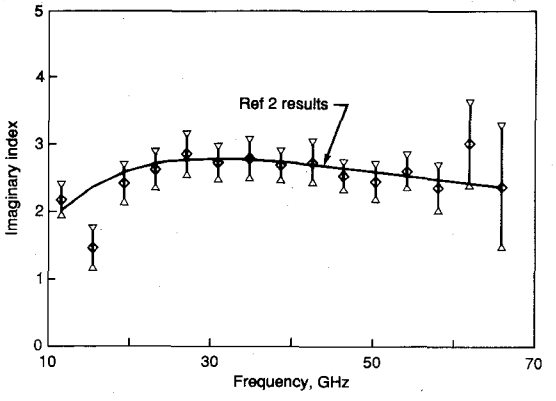

Fig. 10. Imaginary part of complex refractive index for water.

was analyzed using the formulation developed. The plotted values for the index are the means of the values obtained from the fitting procedure for the different data sets. The standard deviation of the values estimates the random electronic component of the uncertainty. Contributions of the sample thickness uncertainty, 0.045 mm, and the window index uncertainty were determined by Monte Carlo analysis. Values for n and k and the total uncertainties are plotted in Figs. 8 and 9. For frequencies above 40 GHz, electronic noise was the principle contributor to the total uncertainty; for lower frequencies, thickness and index errors dominated.

Also plotted in Figs. 8 and 9 are the real and imaginary parts of the refractive index as obtained by the method of travelling waves as reported by Barthel, *et al.* [2]. Values were calculated from the parameters given in Table 1 of [2]. As can be seen, the agreement between these two methods is very good.

In summary, we have presented an extension to the method of coherent microwave transient spectroscopy that allows highly absorptive samples to be characterized and demonstrated the consistency of results so obtained for water with values reported in the literature for other techniques.

Acknowledgment

The authors would like to thank Dr. G. Arjavalingam for helpful discussions regarding the antenna fabrication and Dr. J. L. Freeman, Dr. M. J. LaGasse, and D. L. West for the actual fabrication.

References

[1] G. Arjavalingam, Y. Pastol, J.-M. Halbout, and G.V. Kopcsay, "Broad-band microwave measurements with transient radiation from optoelectronically pulsed antennas," *IEEE Trans. Microwave Theory Tech.*, vol. 28, pp. 615-621, 1990.

[2] J. Barthel, K. Bachhuber, R. Buchner, H. Hetzenauer, "Dielectric spectra of some common solvents in the microwave region: Water and lower alcohols," *Chem. Phys. Lett.*, vol. 165, pp. 369-373, 1990.

[3] A. P. DeFonzo and C. R. Lutz, "Optoelectronic transmission and reception of ultrashort electrical pulses," *Appl. Phys. Lett.*, vol. 51, pp. 212-214, 1987.

[4] Y. Pastol, G. Arjavalingam, J.-M. Halbout, and G. V. Kopcsay, "Characterization of a optoelectronically pulse broadband microwave antenna," *Electron Lett.*, vol. 24, pp. 1318-1319, 1988.

[5] ——, "Coherent broadband microwave spectroscopy using picosecond optoelectronic antennas," *Appl. Phys. Lett.*, vol. 54, pp. 307-309, 1989.

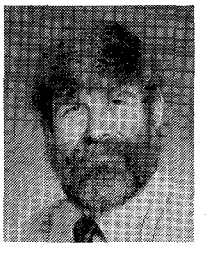

C. David Capps received the B.S. degree in physics from the University of Arkansas, the M.S. and Ph.D. degrees in physics from the Florida State University.

He was a Guest Scientist at the Max Planck Institute for Physics where his research was in experimental particle physics at CERN. In 1977 he joined Hughes Aircraft Company where he worked on propagation of electromagnetic radiation through the atmosphere and modelling performance of imaging infrared systems. He joined Boeing in 1981. Since that time his research areas have included aerosol scattering, optical processing and computing, and electro-optical means of generating and detecting millimeter wave radiation.

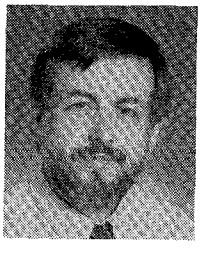

R. Aaron Falk received the B.S., M.S., and Ph.D. degrees in physics from the University of Washington in 1973, 1974, and 1979 respectively.

From 1979 to 1982 he was a Postdoctoral Research Associate at the Joint Institute for Laboratory Astrophysics where he measured fusion related electron-ion collision cross sections in conjunction with Oak Ridge National Laboratory. In 1982 he joined the staff at Ball Aerospace where he initiated a laser radar effort based on coherent detection of the return from a chirped laser diode transmitter. In 1984 Dr. Falk started his current position on the technical staff of the Boeing Company. His research in the area of optical physics has included integrated and fiber optics, optical computing and optical generating of microwaves. This work has led to the issuance of over two dozen patents. He currently leads a group involved in the development of a high power, high speed photoconductor for use in optical generation of microwaves.

Dr. Falk is a member of the American Physical Society, the Optical Society of America and the Puget Sound Chapter of the Optical Society of American and is a Past President of the latter.

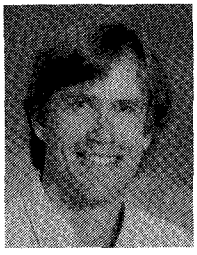

Stuart G. Ferrier received the A.A.S. degree from the University of New Mexico and the certificate in Laser Electro-Optic Technology from Technical Vocational Institute, Albuquerque, NM in 1986.

He has been with the Boeing Company since 1987 where he worked as accelerator operator and optics technician on the Free Electron Laser program. In 1989 he joined the Optical Device Development Lab to work with high speed optoelectronics devices for the generation and study of short pulse microwaves.

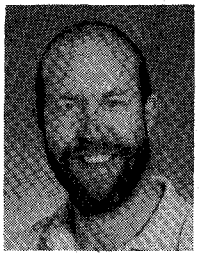

Tim R. Majoch (S'78–M'79) received the B.S. and M.S. degrees in electrical engineering from the University of Washington in 1978 and 1981, respectively. As a graduate student his work centered on control systems for bioengineering applications.

He has since been employed at Boeing in the fields of electrooptics and applied physics. His current position is Coordinator for the Optical Device Development Laboratory in the Boeing Defense and Space Group. His interests include BRDF measurements of materials, single particle optical scattering, optical image processing, radiation effects on optical fibers and control of high temperature furnaces for crystal growing in microgravity environments. His current work is with instrumentation for short pulse laser induced, broad band dielectrometry and optical laser doppler velocimetry of high altitude aerosols.